Astron. Astrophys. 261, 94–104 (1992)

ASTRONOMY AND ASTROPHYSICS

The oblique impact of a high velocity cloud on the galactic disk

F. Comerón and J. Torra

Departament d'Astronomia i Meteorologia, Universitat de Barcelona, Av. Diagonal, 647, E- 08028 Barcelona, Spain

Received August 5, 1991, accepted March 16, 1992

Abstract. The impact on the galactic disk of a large high velocity cloud with a velocity component parallel to the galactic plane is studied in this paper. The galactic disk is assumed to be dominated in volume by the warm, neutral phase, and a cloud model is proposed which is in agreement with the constraints imposed by actual observations. The collision process is followed through 2-D hydrodynamic simulations.

The collision is expected to have some far- reaching consequences for the gas distribution and physical state and the star formation history in the affected region. Some of these consequences should be easily observed if such an impact had taken place near our location in the Galaxy in a recent past; and it seems, indeed, that the origin of the Gould Belt and some of its associated structures may be explained by this mechanism.

Key words: high velocity clouds – galactic structure – interstellar medium – Gould Belt

1. Introduction

The halo- disk interaction in galaxies has been recognized in recent years as an issue of major importance in modelling the physical state and evolution of the galactic interstellar medium (ISM) (see e.g. Cioffi & Shull 1991). The observations of high velocity clouds (HVCs) of neutral hydrogen in the halo of our Galaxy falling towards the galactic disk indicate that this interaction can sometimes take place in a violent way, releasing large amounts of energy in a relatively short time. Some large scale structures are observed in ours and other galaxies which can be interpreted as resulting from the impact of HVCs on the galactic ISM in a recent past (Larson 1972; Mirabel 1982; Heiles 1984; Franco et al. 1988; Tenorio- Tagle and Bodenheimer 1988; Mirabel and Morras 1990).

Obviously, realistic modelling of HVC impacts relies on a good knowledge of the relevant parameters which determine both the initial conditions and the hydrodynamical evolution of the involved material. In the last years, large amounts of information about the physical state and structure of the galactic ISM have accumulated, thanks mainly to the surveys carried out by space based observatories operating in different regions of the electromagnetic spectrum. Parallel to this, increasingly comprehensive and complex models of the large scale behaviour of the ISM have been published which often show remarkably good agreement with the observations.

The situation is less satisfactory in what concerns our knowledge of HVCs, where we have substantial uncertainties derived from the lack of suitable distance indicators associated to them (van Wörden et al., 1985). This prevents us from determining reliable sizes for the HVCs in our Galaxy; because of this, the sizes of the large HVCs that we will consider in this paper are hypothetical. There is no direct evidence that such large clouds are currently being observed falling towards the galactic plane in our Galaxy, although observations do not rule out the possibility that some of the observed clouds may actually be that large. Observations by Mirabel (1982) suggesting a HVC collision in the galactic anticenter may actually involve the existence of rather massive clouds in our Galaxy. On the other hand, very large, massive complexes of high velocity neutral hydrogen have been detected projected on the disk of M 101 (van der Hulst and Sancisi, 1988) which largely exceed the dimensions of the clouds considered in this paper. Thus, we do not find it unreasonable to wonder about the consequences of the collision of a HVC of the proposed size with a galactic disk.

In this paper, we use a realistic, albeit forcedly simplified, model of the galactic ISM and choose the parameters of the impinging HVC within the range allowed by actual observations. The cloud is assumed to fall with a non-zero component of the velocity parallel to the galactic plane. This breaks the axial symmetry which allowed Tenorio- Tagle et al. (1986, 1987) to use a 2-D hydrodynamical code in cylindrical coordinates to study the head-on collision of a HVC with a galactic disk, but, as we will see, the assumption that the cloud is large enough makes it possible to get acceptable results over most of the volume affected by the impact by using a 2-D cartesian code.

2. A model of the galactic ISM

There is a general agreement in that most of the volume of the galactic disk is filled by atomic gas, in three distinct phases characterized by typical densities and temperatures: a hot, ionized medium (HIM), a warm, neutral medium (WNM) and a cold, neutral medium (CNM) (Kulkarni and Heiles, 1988; see also Shull, 1987 and other papers in that volume). On a large scale, the three phases are in rough pressure equilibrium. Transitions among these phases and also the molecular phase govern the overall state of the ISM (Ikeuchi et al., 1984).

Send offprint requests to: F. Comerón

The filling factor of each phase is uncertain. The classical two-phase model (Field et al., 1969) depicts a galactic disk pervaded by the WNM coexisting with embedded cold clouds, where the supernova- originated HIM does not play a primary role. McKee and Ostriker (1977) showed that a self consistent scenario is possible where most of the space is filled by the HIM resulting from supernova explosions throughout the galactic disk. Observations have called into question the validity of the McKee and Ostriker model by indicating that the filling factor of the WNM is significatively higher than predicted (see review by Vladilo, 1989). Recent theoretical results indeed suggest a substantial reduction of the HIM phase filling factor by taking into account the spatial correlation existing among type II supernovae and the possibility that the hot gas escapes into the galactic halo. The "chimney model" developed by Norman and Ikeuchi (1989) seems to predict for the conditions near the solar position in our Galaxy a ISM dominated by the WNM.

We have therefore used in our study a galactic ISM entirely in the WNM phase as a representative approximation to the steady conditions in our region of the galactic disk. The gas density ρ varies with distance to the galactic plane; let us write it in the form:

$$\rho(h) = \rho_0 f(h) \tag{1}$$

ρ_0 is thus the density of the WNM in the galactic plane, and h is the distance to the galactic plane in parsecs. $f(h)$ contains the explicit dependence of ρ on the distance to the galactic plane, for which we have used an expression analogous to the one given by Lockman (1984), but without the terms which introduce a slight asymmetry between the Northern and Southern galactic hemispheres for the sake of simplicity.

Optically thin radiative cooling has been assumed for the gas. For cooling below 10^4 K, we have used the expressions given by Dalgarno and McCray (1972). At temperatures higher than about 10^4 K, rate coefficients for hydrogen excitation and ionization cooling have been taken from Spitzer (1978). Cosmic abundances have been used for metals, with no depletion assumed. Helium-to- hydrogen ratio is assumed to be $Y = 0.1$. The cooling function can be written as

$$\Lambda = \rho^2 l(x, T) \tag{2}$$

where x is the ionization fraction and T is the temperature.

We have used the following simple interstellar heating function:

$$\Gamma = a(h)\rho \tag{3}$$

This expression gives account of the rough proportionality with ρ of the dominant heating mechanisms of the galactic disk (Black, 1987). On the other hand, heating mechanisms are confined to the galactic disk, as for instance cosmic ray heating (Cesarsky, 1980), so we have assumed the dependence of $a(h)$ on h to be of the same form as that of $\rho(h)$.

The condition of thermal equilibrium, $\Gamma = \Lambda$, can be expressed as:

$$a_0\rho_0 f^2(h) = \rho_0^2 f^2(h) l(x, T) \tag{4}$$

Assuming thermal equilibrium, $x = x(T)$, Eq. (4) implicitly gives the equilibrium temperature. We have imposed $T = 8500$ K, a value typical of the WNM (Kulkarni and Heiles, 1988), thus fixing the value of a_0. The independence of Eq. (4) with respect to h makes this model of the vertical structure of the galactic disk isothermal.

Finally, a large- scale magnetic field is introduced in our model. The galactic magnetic field is known to have strong spatial fluctuations, but the existence of a mean value of $B = 3\ \mu$G in the galactic plane with a direction roughly coincident with the galactic rotation seems to be well established (Heiles, 1976). The vertical variation of the magnetic field is poorly known, but as an approximation we will assume a law of the same form as that of the material density (Zweibel, 1987):

$$B(h) = B_0 f(h) \tag{5}$$

3. A model of the HVC

Observational properties of HVCs have been given by Hulsbosch (1975), van Woerden et al. (1985) and de Boer (1989). Several models have been proposed to account for their origin (Oort, 1970; Bregman, 1980; Combes, 1991). It is difficult for a single model to account for all the observed HVCs, and several of them may be simultaneously valid (van Woerden et al., 1985). The entire field of HVCs has been reviewed in depth in a series of recent papers by Wakker (1991) and Wakker and van Woerden (1991).

Attempts to detect HVC absorption lines superimposed on the spectra of distant stars at high galactic latitudes allow to set either upper or lower limits to the distance of the clouds (McGee et al., 1983; Blades et al., 1988; Danly, 1989; Lilienthal et al., 1990). Different results have been obtained; some HVCs seem to lie between the Sun and the background stars, thus being relatively nearby and small. The same seems to be true for some clouds with likely molecular counterparts (Verschuur, 1990). Many other clouds, however, remain undetected in absorption and may thus lie farther away. Haud (1990) has applied to HVCs the 21 cm linewidth-cloud size correlation calibrated for galactic clouds, and has found substantially larger distances up to several kiloparsecs.

Additional evidence for large HVCs falling into galactic disks comes from observations of other galaxies. Besides the already mentioned observations by van der Hulst and Sancisi (1988) in M 101, Rubin and Graham (1990) also have reported the detection of a "drizzle" of high velocity gas into the disk of NGC 4258.

To assign a size and density to our model HVC we have used a "typical" angular diameter of the larger HVCs tabulated by Hulsbosch (1975), assuming that they lie at the mean distance of the clouds listed by Haud (1990). In this way, we obtain a length of about 500 pc. Density has been derived using Hulsbosch's column densities and the quoted cloud length. We use $\rho_c = 10^{-2}$ $M_\odot$ pc^{-3} as a representative value for the cloud. We have assumed the density to be constant throughout the cloud; actually, HVCs are very clumpy and structure is seen in them at all levels of resolution, so the quoted density should represent only an average value. On the other hand, our model cloud has a square cross section for the sake of simplicity, but we have checked that other shapes give very similar results, provided that the initial conditions of size, density and velocity are similar.

Gas temperature in HVCs have been estimated from linewidths (Wakker, 1989). Limits between 30 K and 200 K have been determined, although the thermal contribution to the linewidth is difficult to separate from turbulent motions (Wakker and Schwarz, 1991). To set the initial temperature of the HVC, we have imposed thermal and ionization equilibrium of the gas at its initial position with the chosen density. The same metallicity of the galactic disk has been assumed, as supported by observations by McGee et al. (1983) who find nearly solar abundances for galactic HVCs.

As a value for the velocity of the infalling cloud, we have chosen 100 km s^{-1}, the angle of incidence being 0° (head- on collision) and 45°. After using different values for the velocity and the angle of incidence, we have found these cases to be well representative of the process. For velocities substantially higher than 100 km s^{-1}, the shocks become strong enough so as to photoionize the precursor medium (Shull and McKee, 1979). We will not consider that case here.

The galactic magnetic field is supposed to form an angle of 45° with the computational plane; we have checked that this choice has only a weak influence on the results presented here.

4. Some shock characteristics

The infalling velocity of the HVC is highly supersonical, and in the collision a strongly shocked region develops whose boundaries are front shocks, propagating through both the galactic ISM and the cloud. Simple one- dimensional analytic approximations allow estimations of the involved quantities (Tenorio- Tagle, 1981). In this way, we can estimate the propagation speed of the shock into the cloud, v_s, and consequently the cloud destruction time defined by

$$t_d = \frac{l_c}{v_s} \tag{6}$$

where l_c is the characteristic length of the cloud. Using our input values, we obtain $t_d \cong 15 \cdot 10^6$ yr.

The evolution of the material after the shock crossing is very fast and takes place over a thin region. Within a few hundred parsecs from the plane, the shocked material coming from both the cloud and the galactic ISM evolve much in the same way: inmediately after the shock, a moderately dense, hot region appears where ionization takes place. The ionization of the hydrogen is incomplete and leaves a significant amount of neutral atoms which very efficiently cool down the gas to about 10^4 K, with the subsequent compression to higher density. Below 10^4 K hydrogen excitation cooling ceases to be efficient, but further cooling by collisional excitation of metallic fine structure levels leads to the final compression to the cold equilibrium phase.

A somewhat different behaviour takes place at the beginning of the collision far from the galactic plane. In these regions, the strong density contrast between the cloud and the galactic ISM makes the shock to progress very fast into the galactic disk gas, so that it is heated at very high temperatures and becomes fully ionized. Cooling of this layer finally takes place by free- free radiative transitions, by metal line transitions and by diffusion of the much cooler and neutral gas from the cloud into it. The temperatures somewhat in excess of 10^6 K reached when the shock propagates through the upper galactic disk should produce a significative amount of UV and soft X ray continuum radiation with wavelengths $\lambda > 100$ Å; however, the high opacity of the galactic HI at these wavelengths, combined with the column density lying between the Sun and the upper galactic disk, would make this high energy radiation undetectable.

5. Two-dimensional approach

The computational plane is defined by the cloud direction of motion and the normal to the galactic plane. Let us now assume that our homogeneous cloud has initially the same cross section in all planes parallel to this one and has a finite extent, with a length perpendicular to the computational plane of l_c too. Originally, the cloud is not in pressure equilibrium with the surrounding galactic ISM, and thus a disturbance moves into the sides of the cloud with a speed of the order of the sound speed, c_s (Stone, 1970). As a consequence, by the time t_d, the effects of finite extent have affected a fraction f of the volume of the cloud

$$f = \frac{2c_s t_d}{l_c} = \frac{2c_s}{v_s} \tag{7}$$

Being $v_s \gg c_s$, $f \ll 1$, and thus most of the volume of the cloud remains unaware of this initial pressure imbalance throughout all the collision process. Having assumed that all the cross sections parallel to the computational plane are identical, we shall consider them to evolve all in the same way. This will be a valid representation of the collision process for most of the volume involved in the impact during t_d and beyond, as long as the time elapsed since the beginning of the collision keeps small enough as compared to $0.5 l_c c_s^{-1}$.

Another constraint on the validity of the 2-D approach comes from the differential rotation of the Galaxy, which makes it unappropiate the assumption of a galactic ISM in rest for times of the order of the shearing time, given by the Oort's constant A:

$$t_s = A^{-1} \tag{8}$$

This gives $t_s \cong 10^8$ yr, a less stringent condition than that derived from the finite extent effects. In this paper, we shall consider the evolution of the collision for a time span of $25 \cdot 10^6$ yr, thus allowing us to follow the process well beyond the cloud destruction time while keeping within the constraints imposed by the derived timescales.

6. Numerical methods

The evolution of the impact in the collision plane has been studied by means of a 2-D numerical simulation. We have used a 2-D Eulerian hydrodynamic code in Cartesian coordinates, with shock fronts stabilized by a VonNeumann- type artificial viscosity (VonNeumann and Richtmyer, 1950). The schema is similar to that used by Różyczka (1985). The computational grid we have used is rectangular, with dimensions imposed by the area of the computational plane affected by the impact. This area is estimated at the beginning of the simulation by calculating the displacement of the cloud in a time t_d if it had not encountered the galactic disk.

The computational gris is divided in 128 per 128 cells. This implies a cell size of a few tens of parsecs, which in fact is a distorting factor in our results provided that the post- shock evolution of the material takes place over a much smaller scale and the artificial viscosity spreads out the shocks over a length larger than desirable. However, we still can expect our results to give a valid large scale picture of the process, even though small scale but interesting details are regrettably lost.

Each computational step updates values of the material density ρ, the velocity $\mathbf{v}$, the internal energy density e, the magnetic field $\mathbf{B}$ and the degree of ionization x in each cell, by means of the magnetohydrodynamic equations in Eulerian form modified to allow for an artificial viscosity term:

$$\frac{\partial \rho}{\partial t} = -\rho(\nabla \cdot \mathbf{v}) - (\mathbf{v} \cdot \nabla)\rho \tag{9}$$

$$\begin{aligned}\frac{\partial v_i}{\partial t} = &-\frac{1}{\rho}\frac{\partial p}{\partial r_i} - \frac{1}{\rho}\frac{\partial q_i}{\partial r_i} - (\mathbf{v} \cdot \nabla)v_i - g_i \\ &-\frac{1}{2\rho\mu_0}\frac{\partial}{\partial r_i}\mathbf{B}^2 + \frac{1}{\rho\mu_0}(\mathbf{B} \cdot \nabla)B_i\end{aligned} \tag{10}$$

$$\begin{aligned}\frac{\partial e}{\partial t} = &-p(\nabla \cdot \mathbf{v}) - \sum_{i=1}^{3} q_i \frac{\partial v_i}{\partial r_i} - (\mathbf{v} \cdot \nabla)e - e(\nabla \cdot \mathbf{v}) \\ &+(\Gamma - \Lambda)\end{aligned} \tag{11}$$

$$\frac{\partial B_i}{\partial t} = (\mathbf{B} \cdot \nabla)v_i - B_i(\nabla \cdot \mathbf{v}) - (\mathbf{v} \cdot \nabla)B_i \tag{12}$$

$$\begin{aligned}\frac{\partial x}{\partial t} = &(\epsilon(T)x(1 - x + x_m) - \beta(T)x(x - x_m))\frac{\rho}{(1 + 4Y)m_H} \\ &-(\mathbf{v} \cdot \nabla)x\end{aligned} \tag{13}$$

In these equations, the subscript i denotes the components of a vector, being $\mathbf{r}$ the position. $p = \frac{2}{3}e$ is the pressure, $\mathbf{g}$ is the gravitational acceleration, μ_0 is the magnetic permeability and x_m is the contribution to the ionization fraction from the metals with low ionization potential; in a gas with cosmic abundances, $x_m \cong 5 \cdot 10^{-4}$. $\epsilon(T)$ and $\beta(T)$ are respectively the collisional ionization and recombination coefficients for hydrogen whose expressions are taken from Spitzer (1978). Finally, $\mathbf{q}$ is the artificial viscosity whose components q_i are:

$$q_i = C\rho(\Delta v_i)^2, \qquad \text{if } \Delta v_i < 0 \tag{14a}$$

$$q_i = 0, \qquad \text{if } \Delta v_i > 0 \tag{14b}$$

Δv_i is the difference in the i component of the velocity along the direction r_i between the two cells adjacent to the considered one, and C is an adimensional constant whose value is a few units.

In Eq. (13), only ionization of hydrogen is considered, and the gas is assumed to be composed mainly of hydrogen and helium, with $Y = N_{He}/N_H$.

The gravitational acceleration $\mathbf{g}$ appearing in Eq. (10) is in general due to the mass- dominant stellar galactic disk, for which we have used the force law perpendicular to the galactic plane given by Gilmore (1989). In regions near strong gas density gradients we have also considered the self- gravity of the gas by calculating the resulting force exerted on a cell by its neighbours up to a certain distance. We consider it realistic to neglect the gravitational contribution from the gas lying farther away, since it is small when compared to likely more local, stellar- component-originated perturbations such as nearby pre-existing open clusters or associations.

7. Results

In Figs. 1-2, results in the computational plane are displayed in a grey logarithmic scale for the density, temperature, gravitational instability length and ionization fraction. The adopted gravitational instability length is just an approximation in which each cell is treated as if it was located at the midplane of an infinite, plane- parallel, self- gravitating isothermal layer with midplane density ρ, temperature T and mean mass per particle μ; in this case, the gravitational instability length is given by

$$L_g = 3.47\sqrt{\frac{T}{\mu\rho}} \tag{15}$$

where L_g is in parsecs, T in K and ρ in $M_\odot$ pc^{-3} (Larson, 1985). Perturbations with longer wavelengths are unstable against gravitational collapse. The gravitational instability maps in Figs. 1 and 2 should be regarded as displaying the probability of star formation, black corresponding to the highest probability and white to the lowest.

The general outline of the process is the same both in the head-on collision and in the oblique collision: from the beginning, a shocked region develops where density and temperature increase and ionization takes place. The shocked region is initially very hot but, as time runs, cooling begins to dominate and a dense, cold, neutral layer results where star formation is likely to take place.

The cold, dense region actually appears within a few thousand years since the beginning of the collision, but because of its thinness it becomes visible in the figures only when it has grown up to about the size of a computational cell, after several million years. In the final stages of the process, the three zones of the shock described before (initial hot, transition warm and equilibrium cold) can be clearly distinguished in the figures.

A significative and interesting difference appears between the cases of head- on and oblique collisions. In the head- on collision, the compressed material lying between the two front shocks remains trapped there and can escape only through the boundaries of this region with a speed of the order of that of the sound. This makes the flow of material outwards from the shocked region very slow. The situation changes when the collision is oblique, because in that case the material entering the shocks has a velocity component parallel to the shock surfaces in their reference frame, and thus there exists an appreciable flow of compressed material escaping from the shocked layer. This material is slowed down by the surrounding gas of the unperturbed galactic disk and finally appears as roughly outlining the path followed by the shocked region through the galactic disk.

The resulting distribution of the cool, dense material is determined by the vertical density profile of the galactic disk, as the deceleration of the shocked layers depends on the density they find along their path. In this way, the initial bow shock is

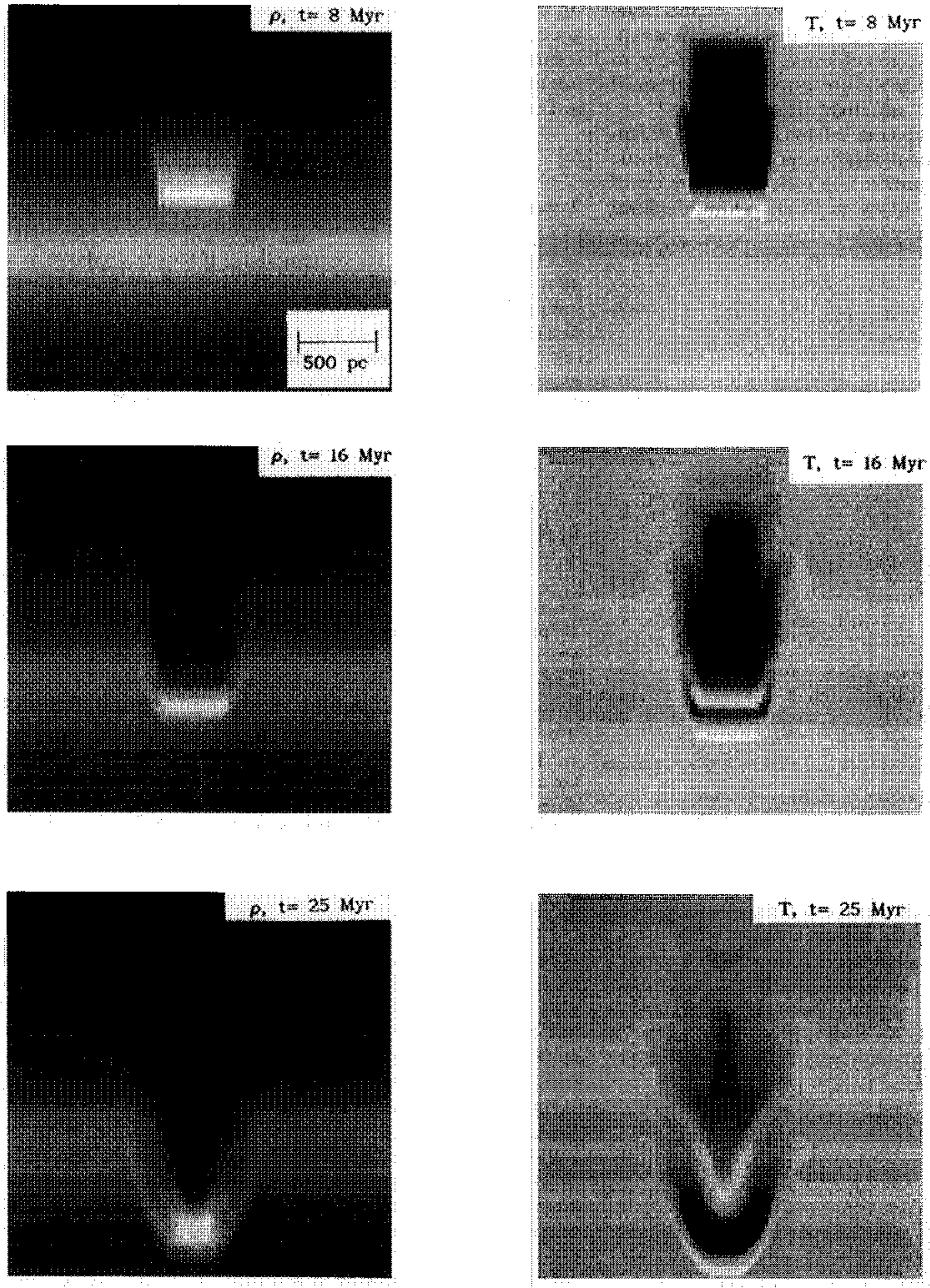

Fig. 1a. Time evolution of the density ρ and the temperature T for an angle of incidence of 0° (head- on collision). The top frames show the region after $8 \cdot 10^6$ yr, the middle ones at $16 \cdot 10^6$ yr and the bottom ones at $25 \cdot 10^6$ yr. Each frame covers an area 2700 pc per 2700 pc perpendicular to the galactic plane.

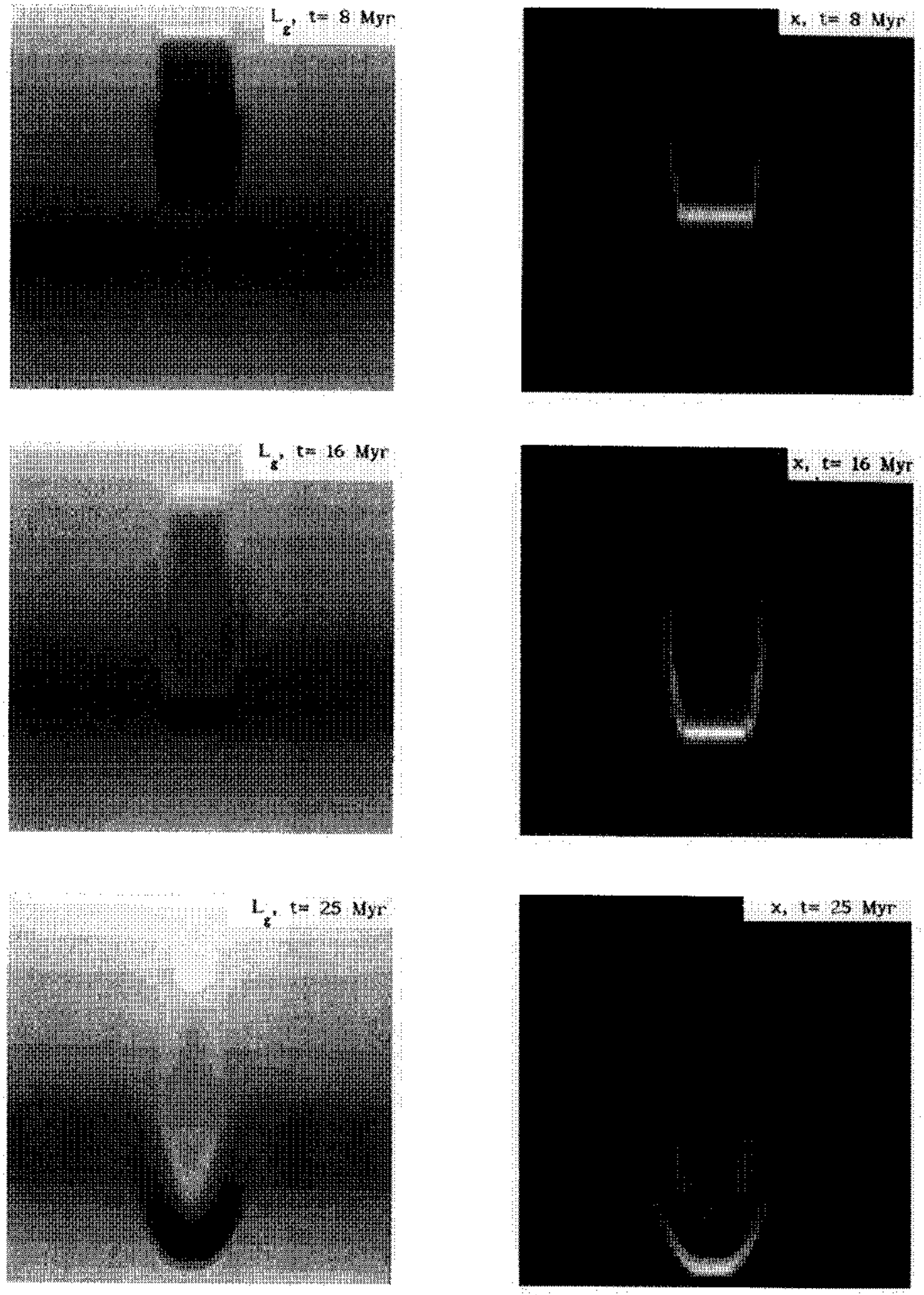

Fig. 1b. Time evolution of the gravitational instability length L_g and the ionization fraction x for an angle of incidence of 0° (head- on collision). The top frames show the region after $8 \cdot 10^6$ yr, the middle ones at $16 \cdot 10^6$ yr and the bottom ones at $25 \cdot 10^6$ yr. Each frame covers an area 2700 pc per 2700 pc perpendicular to the galactic plane.

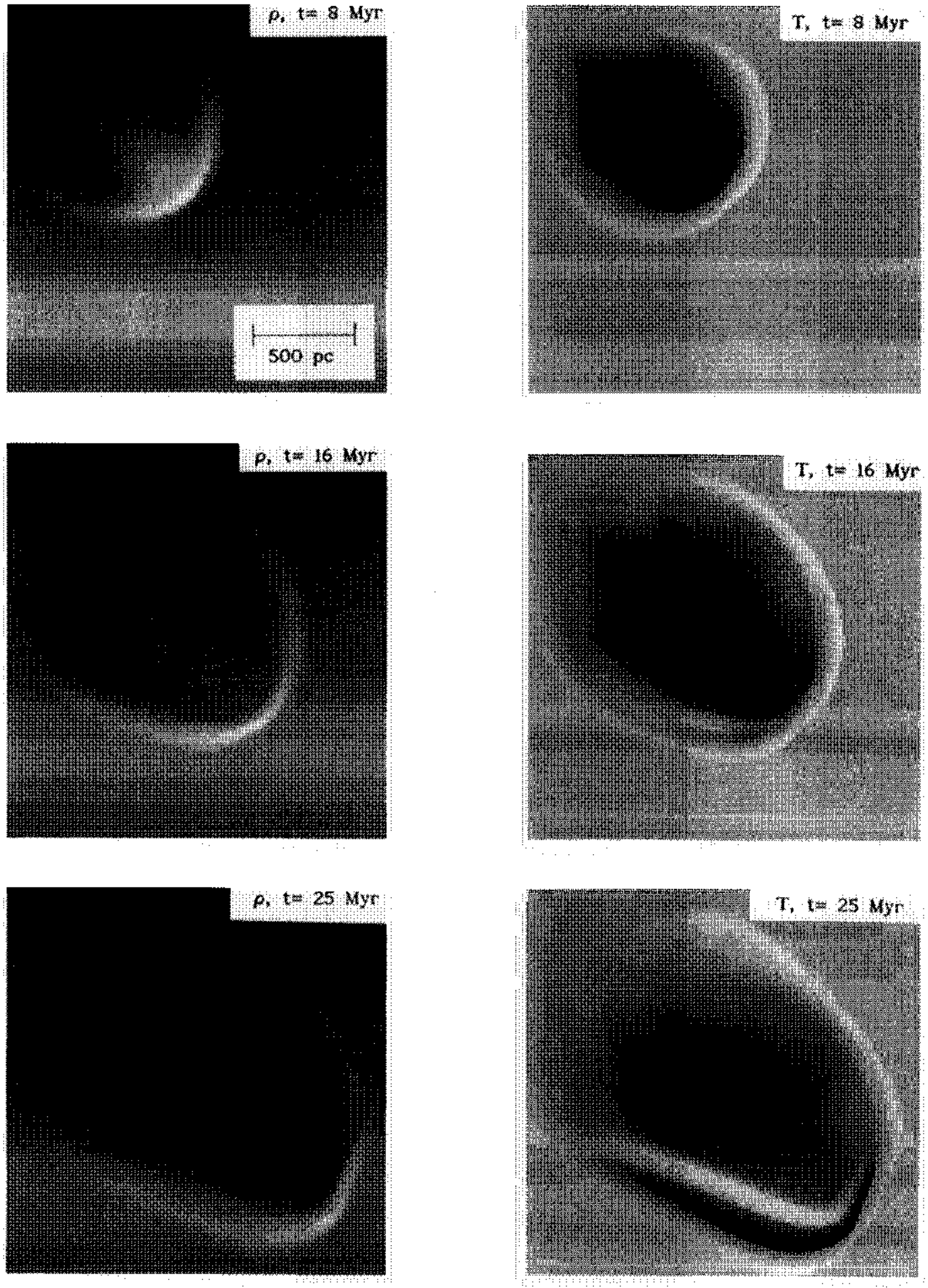

Fig. 2a. Time evolution of the density ρ and the temperature T for an angle of incidence of 45°. The top frames show the region after $8 \cdot 10^6$ yr, the middle ones at $16 \cdot 10^6$ yr and the bottom ones at $25 \cdot 10^6$ yr. Each frame covers an area 2200 pc per 2200 pc perpendicular to the galactic plane.

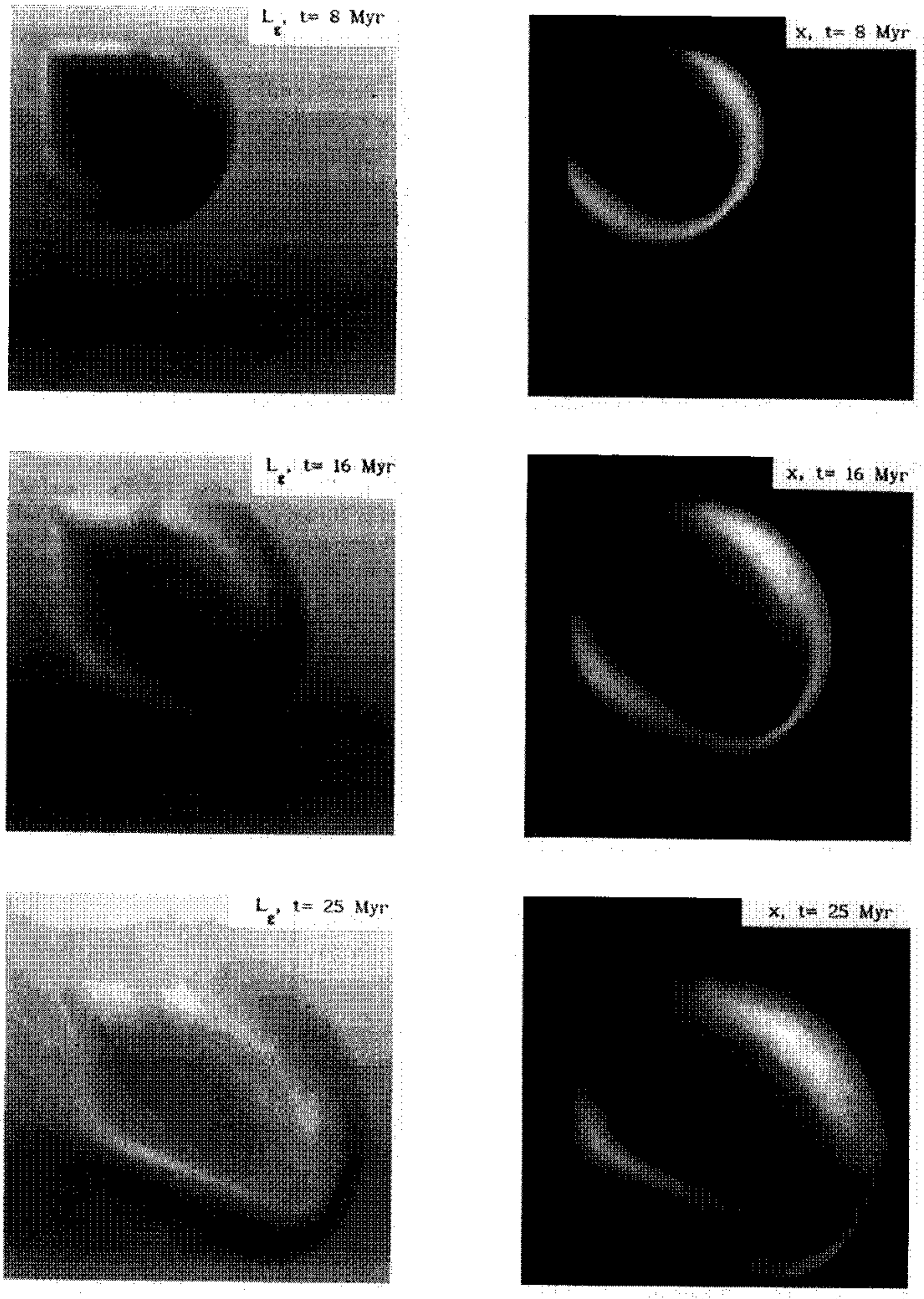

Fig. 2b. Time evolution of the gravitational instability length L_g and the ionization fraction x for an angle of incidence of 45°. The top frames show the region after $8 \cdot 10^6$ yr, the middle ones at $16 \cdot 10^6$ yr and the bottom ones at $25 \cdot 10^6$ yr. Each frame covers an area 2200 pc per 2200 pc perpendicular to the galactic plane.

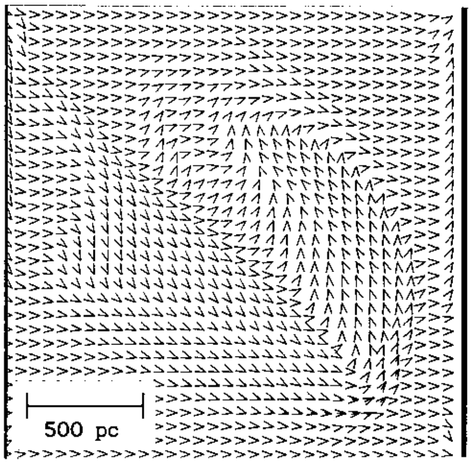

Fig. 3. Distribution of the magnetic field in the computational plane after 25 million years for a representative case. The angle of incidence of the cloud and the angle between the magnetic field and the computational plane are both 45°

distorted giving the $V-$ shapes which can be seen in the last frames of Figs. 1-2.

In the densest regions of the galactic disk, where the compression is strongest, the material escaped from the shock fronts further evolves towards the cold equilibrium phase and recombines, thus giving an extended region with a small gravitational instability length tilted with respect to the galactic plane. The gas escaped from the shocked regions at greater distances over the galactic plane is not so much compressed, and the lower density makes its thermal and ionization evolution much slower. As can be seen in Figs. 1-2, a large, partially ionized, warm volume similar to a fossile HII region is expected to survive long after it has been affected by the collision. In addition, the horizontal motions on the right- hand side of the bow shock in our figures are slowed down by the high gas densities near the galactic plane, thus resulting in a roughly vertical layer of compressed gas connecting the galactic plane with the central part of the bow shock which has crossed it. Furthermore, the drag force from the galactic disk gas and the gravitational force from the stellar disk finally stop this central region when it is several hundred parsecs below the galactic plane. As this happens after a time where the fraction f, as defined by Eq. (7), is not much smaller than one, the condition for our two- dimensional approximation to be valid is not fulfilled, and this stage is not shown in the figures.

The final velocities of the shocked regions with respect to the rest galactic disk are much smaller than the initial cloud velocity, but small kinematical peculiarities would still be expected in the stars formed by this process. A large scale disturbance in the galactic magnetic field also appears in our results (Fig. 5), although, as we have indicated before, the assumption of a smooth, structurally simple galactic magnetic field is a rather naive oversimplification, far from the observed reality which may easily mask the predicted effect on it of the cloud collision.

In some of our numerical experiments, the magnetic field, the self- gravity of the gas of the gravity of the galactic disk have been removed. These physical effects, and especially the first two, are expected to substantially influence the further evolution of the resulting dense layers. Nevertheless, comparison between models which do and do not include them shows that none of them plays a significant role neither in the large scale configuration of the region affected by the collision nor in the firsts stages of its further evolution. In the case of the magnetic field, the large scale distribution of the material and its physical conditions after the shock are virtually the same regardless of the field orientation; this is why we present in Figs. 1-2 results only for an angle of 45° between the galactic magnetic field and the collision plane.

8. A possible origin of the Gould Belt

Some of the predictions of the model we have discussed so far show a striking coincidence with observations of the distribution of young objects near the Sun. The local system of O and B stars has been known for more than a century to show a concentration towards a plane tilted about 20° with respect to the galactic plane, whose nodes are roughly aligned with the galactic rotation direction (Fig. 4). This structure is known as the Gould Belt (Lesh, 1968; Stothers and Frogel, 1974; Lindblad, 1974). Large molecular clouds and dark clouds also show an evident trend to concentrate along this plane (Lindblad et al., 1973; Dame et al., 1987; Taylor et al., 1987). Franco et al. (1988) already suggested that the Orion and Monoceros molecular complexes may have formed as a result of the impact of a HVC. Similar suggestions relating the Gould Belt and the infalling of halo material have been made by Weaver (1974) and Gómez de Castro (1991). Strauss et al. (1979) and Cappa de Nicolau and Pöppel (1986) have found the existence of significant amounts of cold, dense neutral hydrogen in association with the Belt. The stars in the Gould Belt are also known to show kinematic peculiarities (Lesh, 1968; Frogel and Stothers, 1977; Westin, 1985; Comerón and Torra, 1991; Comerón et al., 1992) which apparently consist of an expanding motion.

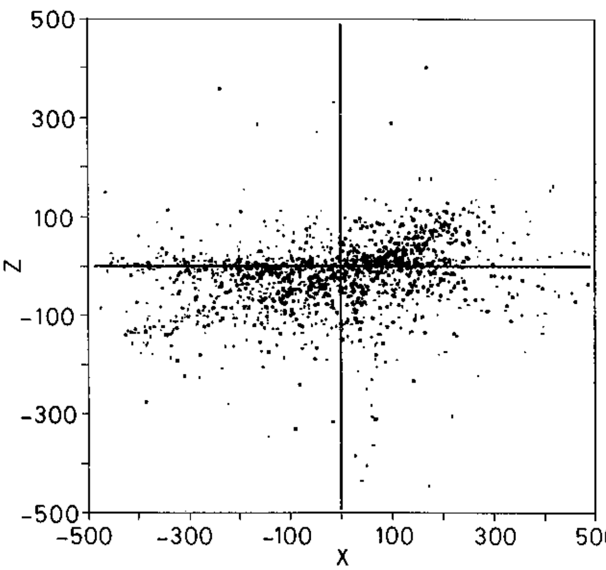

Fig. 4. Spatial distribution of O and B stars projected on a plane perpendicular to the galactic plane. x is directed towards the galactic center, z towards the galactic pole. Distances are in parsecs. The sample of stars plotted here has been described in Comerón et al. (1992)

Both the tilt and the particular kinematics of the Gould Belt suggest the possibility that it was formed in a recent past by the collision with the galactic disk in the solar neighbourhood

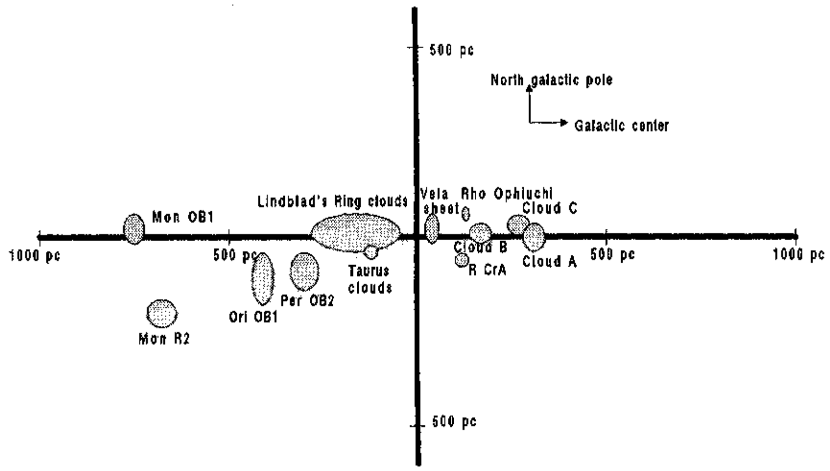

Fig. 5. Spatial distribution of some molecular clouds in the solar neighbourhood, projected on a plane perpendicular to the galactic plane. x is directed towards the galactic center, z towards the north galactic pole. Data were taken from Dame et al. (1987)

of a HVC coming from inside the solar circle and from above the galactic plane, similar to the clouds described as population N by Wakker and van Wörden (1991). Additional evidences seem to support this hypothesis: as expected from our results, the Gould Belt is clearly asymmetric, extending farther from the galactic plane below it than above it. The region shown in Fig. 4 would rather correspond to the parts of this structure closest to the Sun, the lower end of the Gould Belt in Fig. 4 corresponding to stars in the Orion OB1 association. There are indications, however, that Gould Belt associated objects can be found farther away; the active star forming region Monoceros R2, for instance, is at about the same distance below the galactic plane as Orion OB1 (Maddalena et al., 1986). It is suggestive to regard Orion OB1 and Monoceros R2 as tracers of the lowest end of the shocked region (Fig. 5), while the high density rift going up to almost vertically from this lowest end might be the Northern and Southern filaments identified by Maddalena et al. (1986), the former including the Rosetta nebula complex. They intersect the galactic plane in the area where the OB asociations Monoceros OB1 and Canis Major OB1 are observed (Eggen, 1978). Needless to say, this geographical identification of actually observed features with our model predictions is just speculative, but in out opinion the noted consistence should deserve some attention.

Further developments in our model are required in order to include the fragmentation processes leading to the formation of large scale structures such as star forming complexes and OB associations (Elmegreen, 1987; Franco et al., 1988), whose locations, sizes, masses and evolutionary timescales could be compared to actual observations of the Gould Belt. The chosen input parameters of the infalling cloud presented here are able to reproduce the overall extent of the Belt. In addition, estimates from our model predict a total mass for the compressed region of 10^7 $M_\odot$; this is about the total mass in molecular complexes associated to the Gould Belt (Dame et al., 1987), thus indicating a high efficiency in the transformation of atomic to molecular gas. Strauss et al. (1979) reached this same conclusion from their observations of atomic hydrogen, which they estimated to be only $\cong 7\%$ of the total mass of the Belt.

The existence of an extended partially ionized, low density region appearing in our model above the galactic plane is difficult to check observationally. In principle, such a region should be emitting thermal bremsstrahlung radiation and optical recombination lines, and it may appear as a statistical increment in the dispersion measures of pulsars whose line of sight passes through it. Unfortunately, the low densities difficult detection in practice. The Hα expected intensity in Rayleigh, taking as representative values $n_e^2 \cong 10^{-3}$ cm^{-6}, $T \cong 10^4$ K, $l \cong 200$ pc, should be (Kulkarni and Heiles, 1988):

$$I \cong 1.4 \cdot 10^3 n_e^2 T^{-0.9} l \cong 0.07$$

This is below the detection limit of the Hα survey carried out by Reynolds (1984), and represents only a small fraction of the galactic Hα background. Similar problems occur with the thermal bremsstrahlung radiation. The survey of pulsars by Lyne et al. (1985) does not show any significative trend in this respect neither.

Finally, we should mention that an apparently local deformation of the galactic magnetic field, associated to the well known North Polar Spur, is well established by observations. This deformation may be related to the perturbation induced by the HVC impact, as illustrated in Fig. 3.

9. Conclusions

The oblique impact of a large high velocity cloud with the galactic disk is shown to produce an important redistribution of the gaseous mass and gas phase transitions in the affected region, and is able to give rise to extended dense, cold, potential star forming regions. Star formation would be one of the most easily observable consequences, with some anomalous features such as high galactic latitude star formation or kinematical peculiarities. The observed characteristics of the Gould Belt and possibly associated objects such as Monoceros R2 are strongly reminiscent of these anomalous features. In addition, some of the HI supershells discussed by Heiles (1984) may have been formed by such mechanisms, and the magnetic field associated to the North Polar Spur may be the record of the disturbance caused on the galactic magnetic field by the oblique collision. Other predictions of the model are more difficult to test experimentally, such as the existence of an extended ionized volume high above the galactic plane.

Further work is currently under way mainly to study the time evolution of the galactic plane- crossing dense region, with the aim of making some reliable predictions on the characteristics of star formation in it.

Acknowledgements. We are pleased to acknowledge help and discussions with Dr. Ana E. Gómez and the valuable comments from the referee leading to the improvement of this paper. This research is supported by the CICYT under contract ESP88-0731 and Acciones Integradas Hispano- Francesas. FC also acknowledges the CIRIT for financial support at the early stages of this work.

References

Black, J.H, 1987, in: Interstellar Processes, eds. D.J. Hollenbach and H.A. Thronson, D.Reidel Publ. Co.
Blades, J.C., Wheatley, J.M., Panagia, N., Grewing, M., Pettini, M., Wamsteker,W., 1988, ApJ 332, L75
de Boer, K.S., 1989, in: Structure and Dynamics of the Insterstellar Medium, eds. G. Tenorio-Tagle, M. Moles and J. Melnick, Springer-Verlag
Bregman, J.N., 1980, ApJ 236, 577
Cappa de Nicolau, C.E., Pöppel, W.G.L., 1986, A&A 164, 274
Cesarsky, C.J., 1980, ARA&A 18, 289
Cioffi, D., Shull, J.M., 1991, ApJ 367, 96
Combes, F., 1991, A&A 243, 109
Comerón, F., Torra, J., 1991, A&A 241, 57
Comerón, F., Torra, J., Gómez, A.E., 1992, Ap&SS 187, 187
Dalgarno, A., McCray, R.A., ARA&A 10,375
Dame, T.M., Ungerechts, H., Cohen, R.S., de Geus, E.J., Grenier, I.A., May, J., Murphy, D.C., Nyman, L.-Å, Thaddeus, P., 1987, ApJ 322, 706
Danly, L., 1989, ApJ 342, 785
Eggen, O.J., 1978, PASP 90, 436
Elmegreen, B.G., 1987, ApJ 312, 626
Field, G.B., Goldsmith, D.W., Habing, H., 1969, ApJ 155, L49
Franco, J., Tenorio-Tagle, G., Bodenheimer, P., Różyczka, M., Mirabel, I.F., 1988, ApJ 333, 826
Frogel, J.A., Stothers, R., 1977, AJ 81, 890
Gómez de Castro, A.I.: 1991, in: Evolution of Interstellar Matter and Dynamics of Galaxies, ed. J. Palous (in press)
Gilmore, G, 1989, in: The Milky Way Galaxy, 19th Saas-Fee Course, eds. R. Buser and I. King, Geneva Observatory
Haud, U., 1990, A&A 230, 145
Heiles, C., 1976, ARA&A 14, 1
Heiles, C., 1984, ApJS 55, 585
Hulsbosh, A.N.M., 1975, A&A 40, 1
van der Hulst, T., Sancisi, R., 1988, AJ 95, 1354
Ikeuchi, S, Habe, A., Tanaka, Y.D., 1984, MNRAS 207, 909
Kulkarni, S.R., Heiles, C., 1988, in: Galactic and Extragalactic Radio Astronomy, eds. G.L. Verschuur and K.I. Kellerman, Springer-Verlag
Larson, R.B., 1972, Nat 236, 21
Larson, R.B., 1985, MNRAS 214, 379
Lesh, J.R., 1968, ApJS 151, 371
Lilienthal, D., Meyerdierks, H., de Boer, K.S., 1990, A&A 240, 487
Lindblad, P.O., 1974, in: Stars and the Milky Way System, ed. L.N. Mavridis, Springer-Verlag
Lindblad, P.O., Grape, K., Sandqvist, Aa., Schober, J., 1973, A&A 24, 309
Lockman, F.J., 1984, ApJ 283, 90
Lyne, A.G., Manchester, R.N., Taylor, J.H., 1985, MNRAS 213, 613
Maddalena, R.J., Morris, M., Moscowitz, J., Thaddeus, P., 1986, ApJ 303, 375
McGee, R.X., Newton, L.M., Morton, D.C., 1983, MNRAS 205, 1191
McKee, C.F., Ostriker, J.P., 1977, ApJ 211, 135
Mirabel, I.F., 1982, ApJ 256, 112
Mirabel, I.F., Morras, R., 1990, ApJ 356, 130
vonNeumann, J., Richmyer, R.D., 1950, J. Appl. Phys. 21, 232
Norman, C.A., Ikeuchi, S., 1989, ApJ 345, 372
Oort, J.H., 1970, A&A 7, 381
Reynolds, R.J., 1984, ApJ 282, 191
Różyczka, M., 1985, A&A 143, 59
Rubin, V.C., Graham, J.A., 1990, ApJ 362, L5
Shull, J.M., 1987, in: Interstellar Processes, eds. D.J. Hollenbach and H.A. Thronson, D. Reidel Publ. Co.
Shull, J.M., McKee, C.F., 1979, ApJ 227, 131
Spitzer, L., 1978, Physical Processes in the Interstellar Medium, J. Wiley
Stone, M.E., 1970, ApJ 159, 277
Stothers, R., Frogel, J.A., 1974, AJ 79, 1974
Strauss, F.M., Pöppel, W.G.L., Vieira, E.R., 1979, A&A 71, 319
Taylor, D.K., Dickman, R.L., Scoville, N.Z., 1987, ApJ 315, 104
Tenorio-Tagle, G., 1981, A&A 94, 338
Tenorio-Tagle, G., Bodenheimer, P., 1988, ARA&A 26, 145
Tenorio-Tagle, G., Bodenheimer, P., Różyczka, M., Franco, J., 1986, A&A 170, 107
Tenorio-Tagle, G., Franco, J., Bodenheimer, P., Różyczka, M., 1987, A&A 179, 219
Verschuur, G.L., 1990, ApJ 361, 497
Vladilo, G., 1989, in: Evolutionary Phenomena in Galaxies, eds., J.E. Beckman and B.E.J. Pagel, Cambridge Univ. Press
Wakker, B.P., 1989, in: Structure and Dynamics of the Interstellar Medium, eds. G. Tenorio-Tagle, M. Moles and J. Melnick, Springer-Verlag
Wakker, B.P., 1991, A&A 250, 499
Wakker, B.P., Schwarz, U.J., 1991, A&A 250, 484
Wakker, B.P., van Wörden, H., 1991, A&A 250, 509
Weaver, H., 1974, in: Highlights of Astronomy, ed. G. Contopoulos, D. Reidel Publ. Co.
Westin, T.N.G., 1985, A&AS 60, 99
van Woerden, H., Schwarz, W.J., Hulsbosch, A.N.M., 1985, in: The Milky Way Galaxy, eds. H. van Woerden, D.J. Allen and W.B. Burton, IAU Symp. 106, D. Reidel Publ. Co.
Zweibel, E.G., 1987, in: Interstellar Processes, eds. D.J. Hollenbach and H.A. Thronson, D. Reidel Publ. Co.

This article was processed by the author using Springer-Verlag TEX A&A macro package 1991.